Sensor-Less Detection of Wheel Alignment Error for a Wheeled Mobile Robot using the Disturbance Observer

Shiva Paudel
Industrial Systems Engineering
Asian Institute of Technology
Bangkok, Thailand
paudel.shiva1996@gmail.com

A. M. Harsha S. Abeykoon
Department of Electrical Engineering
University of Moratuwa
Moratuwa, Sri Lanka
harsha@uom.lk

S. D. Arunya P. Senadeera
Industrial Systems Engineering
Asian Institute of Technology
Bangkok, Thailand
arunyasenadeera@gmail.com

***Abstract*—Estimating the wheel camber error is a challenging task without attaching an additional sensors or mechanisms on the Electrical vehicles. Almost all the electrical automobiles are using several combinations of sensors to detect the camber errors, toe in/out errors and other wheel conditions measurements. This paper introduces a simple method to identify the camber and toe in/out error using disturbance observer(DOB) without using any additional sensors or mechanisms. Proposed concept is practically demonstrated by using a differential drive mobile robot. The Wheeled mobile robot (WMR) is commanded to run on a predefined path and torque profile is observed to identify whether wheels of the vehicles are misaligned.**

***Keywords*—camber errors, toe-in/out errors, disturbance observer(DOB), Sensor-less, reaction torque observer(RTOB), Wheeled mobile robot**

I. INTRODUCTION

The camber, or relative inclination is defined as the wheel plane to the perpendicular to the carriageway, is significant for tracking and steering. Negative camber defined as the top of the wheel is tilted towards the vehicle, whereas positive camber tilts the top of the wheel away from the vehicle. The camber is significance when reducing the turning circle of the vehicle and tire wear. The camber adjustments in commercial vehicles, particularly graders, are usually applied to a camber cylinder mounted on a front swing axle, which aligns with the wheel pivot unit by moving in and out. Adjustment of the camber angle has hitherto been manual [1]. The camber angle of each wheel improves the vehicle maneuverability and stability index and also minimizing energy consumption.

Takamasa et al. proposed a method to improvement of posture stabilization for a two-wheel electric motorcycle considering the camber angle [2]. The proposed method is simulation only and too complex for four wheeled vehicles. He Xu et al. developed a kinematic model, based on caster and camber for an articulated all-terrain rover [3]. But it assumed that there is no deformation of wheels as well as terrain surface. In real world application there is a deformation on both wheel and terrain which results changes in wheel radius. J.Yunta et al. proposed a method to measure the tire strain dynamic behavior based on vertical load, slip angle and the camber angle [4]. Strain gages were attached on the inner of the tire tread. Tire was placed on a drum considering a constant camber angle. Further more authors are willing to achieve estimation of camber angle in future studies. Mounting sensors in tires can be changed it's inertia and consuming the space.And also it needs an extra circuitry to convert the data.

C. Lamy et al. presented a vision-based approach to estimate the wheel camber angle. Camera is mounted on the wheel and it was able to track the tyre- road contact patch that was created by the laser [5]. The wheel camber angle and tyre radius loaded was computed in post processing. An extra mechanism is needed to mount the camera. Such high precision errors need to be calibrated often. J. S. Young et al. proposed an approach to the camber angle measurement for vehicle wheel alignment using 3-axis accelerometer. The 3-axis accelerometer needed to be mounted on the wheel to acquire gravity, and applied the coordinate transformation between the camber inspection system and the vehicle [6]. Accelerometer data is noisy and signal filters are needed. Start up calibration is needed to acquire reliable data.

This Paper is organized as follows. In section II driven wheel kinematics is derived. In section III WMR dynamics is defined. Further, rolling resistance and reaction force is described. Then, the control algorithm is illustrated in section IV. The experimental results are shown in section V. Finally the paper is concluded in section VI.

II. WMR KINEMATICS

To determine whether the wheel of vehicle is perfectly aligned or not we have to derive a kinematics and dynamics models of the mobile robot. Following section covers the kinematics and dynamics of WMR and Dynamics of different misaligned wheel WMR.

Velocity and displacement in WMR were obtained from wheel's motor angular displacement. Therefore, the wheel's

978-1-7281-9975-7/20/$31.00

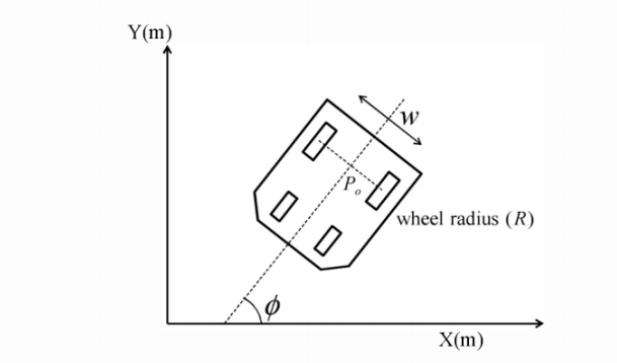

Fig. 1: Wheeled Mobile Robot (WMR) in global Co-ordinate System

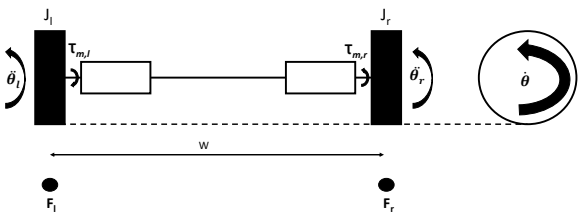

Fig. 2: Wheeled Mobile Robot(WMR) and reaction force in wheels

angular velocity and displacement were converted into global coordinates using following set of kinematic equations.

$$\theta = \begin{bmatrix}\theta_l & \theta_r\end{bmatrix}^T \tag{1}$$

$$X = \begin{bmatrix}x & y & \phi\end{bmatrix}^T \tag{2}$$

$$\dot{X} = J_{aco} \cdot \dot{\theta} \tag{3}$$

Figure 1 shows the WMR in global co ordinate system. Robot position was considered to be at the center of robot's two wheels (P_0). Here, ϕ is the attitude angle that is angle formed between axis perpendicular to mobile robot and x-axis. From equation (1) to (7) defines the forward and inverse kinematics of WMR. $J_{aco} = \begin{bmatrix}\frac{R\cdot\cos\phi}{2} & \frac{R\cdot\cos\phi}{2} \\ \frac{R\cdot\sin\phi}{2} & \frac{R\cdot\sin\phi}{2} \\ \frac{R}{W} & \frac{-R}{W}\end{bmatrix}$

$$\dot{\theta} = J^+_{aco}(\phi) \cdot \dot{X} \tag{4}$$

$$\ddot{\theta} = J^+_{aco}(\phi) \cdot \ddot{X} + \dot{J^+_{aco}}(\phi) \cdot \ddot{X} \tag{5}$$

$$J^+_{aco} = \frac{1}{R}\begin{bmatrix}\cos\phi & \sin\phi & \frac{W}{2} \\ \cos\phi & \sin\phi & \frac{-W}{2}\end{bmatrix} \tag{6}$$

$$\ddot{\theta} = J^+_{aco}(\phi) \cdot \ddot{X} \tag{7}$$

Current position and attitude angle of WMR can be estimated by using dead reckoning. To completely define current position and attitude angle, velocity, angular displacement and previous position were used. Equations (8) and (9) demonstrate how current position of the WMR can be estimated [8].

$$X_k = X_{k-1} + V_{P,k} \cdot \cos(\frac{\phi_k + \phi_{k-1}}{2}) \cdot \Delta t \tag{8}$$

$$y_k = y_{k-1} + V_{P,k} \cdot \sin(\frac{\phi_k + \phi_{k-1}}{2}) \cdot \Delta t \tag{9}$$

Where, V_p is the WMR velocity in global coordinate system, Δt is the sampling time.

The attitude angle of the WMR can be calculated using equation (10).

$$\phi = \frac{R}{W} \cdot (\theta_r - \theta_l) \tag{10}$$

III. WMR Dynamics

The motion of WMR was created by the torque generated in each wheel by its respective motors. WMR's dynamic is important to analysis when it is in contact with its environment. To evaluate the wheel alignment, the dynamics of the WMR plays an important role. In this section, the dynamics of the WMR will be discussed and change of dynamical properties with several wheel misalignment will be discussed.

A. Normal WMR

Figure 7d shows the basic diagram of traction force generation for mobility of WMR. Centre of Gravity of the mobile robot was considered to be centered between two driving wheels. The traction forces on wheels create the forward moment to the mobile platform. The generated shear force in contact is acting between rolling wheel and the surface equals to the traction force. It is assumed that there is no slip in wheels which means that wheel and the ground contact point is instantaneously stationary. Viscous friction was also neglected as it was not significant.

In the figure 7d $\ddot{\theta_r}$ and $\ddot{\theta_l}$ are right and left wheel acceleration, $\tau_{m,r}$ and $\tau_{m,l}$ are respective wheels torques. J is moments of inertia of the robot whereas J_r and J_l are respective wheel's moment of inertia. The forces F_r and F_l going into the planes are right and left wheel frictional forces. Equation (11) defines the relation between wheel torque and the angular acceleration of the wheels.

$$\tau = M_\theta \cdot r^2 \cdot \ddot{\theta} \tag{11}$$

where,

$$\tau = \begin{bmatrix}\tau_{m,r} & \tau_{m,l}\end{bmatrix}^T \tag{12}$$

$$\ddot{\theta} = \begin{bmatrix}\ddot{\theta_r} & \ddot{\theta_l}\end{bmatrix}^T \tag{13}$$

$$M_\theta = \begin{bmatrix}(\frac{J}{W^2} + \frac{M}{4} + \frac{J_r}{r^2}) & (\frac{M}{4} - \frac{J}{W^2}) \\ (\frac{M}{4} - \frac{J}{W^2}) & (\frac{J}{W^2} + \frac{M}{4} + \frac{J_l}{r^2})\end{bmatrix} \tag{14}$$

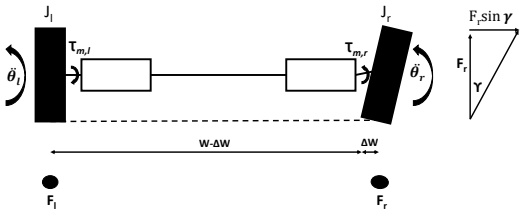

Fig. 3: WMR with wheels reaction forces and frictional forces when one wheel is cambered

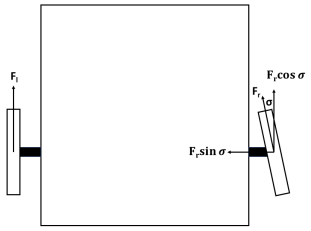

Fig. 4: Lateral force and loss in WMR when one wheel is TOE-IN

B. WMR with Wheels Misaligned

Sometimes wheels might get misaligned suddenly. To find out the wheel misalignment in IC automobiles there has been several mechanical as well as electrical development since the development of automobiles. However when it comes to the electric automobiles or wheeled robots using similar driving technology. If the wheels are misaligned, a similar torque variation is visible and it could be detected using the motor current. In this section dynamics of wheeled mobile robot was discussed so that we can find out any misalignment without any sensor.

1) Reaction Force and Slip: The frictional force in robot's wheel is dependent on the load that is being applied on it. Therefore, reaction force plays an important role when it comes to wheel alignment. Wheel camber changes the load on the wheel. Wheel toe-in/out changes the forward frictional force as discussed in the following sections. These changes in reaction force and frictional force, ultimately affect the torque required to keep the robot on the planned path. The wheel misalignments create constant sideways forces as shown in the Figures 3 and 4. When robot is moving in a straight path, the cambered wheel will have to do more work than the non cambered wheel which allows us to determine whether the wheel is perfectly aligned or not.

Figure 3 shows the generation of traction force for mobility of one wheel cambered WMR. It is assumed that there was no significant change in Center of Gravity (COG) before and after the wheel being cambered. The angle γ defines the angle of wheel camber in the wheel.$\tau_{m,l}$ and $\tau_{m,r}$ are the generated wheel torque. F_r and F_l are the frictional force alongside the direction of the wheel movement.

Consider the mass of the robot platform to be M, Inertia of the robot around Z-axis to be J and wheels inertia to be J_l and J_r for left and right wheel respectively.

The dynamic equations for left and right wheel as defined in equation (14) can be used to monitor the torque in each wheel of the platform. Consider when the right wheel of WMR is cambered as in the Figure **??**. Now the cambered wheel has to work more than the non-cambered left wheel in order to keep the robot in the planned path when it is going on straight path. It is straight forward to determine whether there is a problem of wheel alignment when the robot is moving on a straight path. However, assuming all paths to be straight is far from the reality. Real life electrical vehicles will be moving in highways with variations of turns. Determining whether any wheel is taking more than require torque while its moving in a curvature is challenging. Simplest and most effective way to overcome this problem is to redefine the ratios of wheel torques required to take variety of turns while the wheels are in perfect conditions.

The Figure 4 shows another variation of wheel misalignment i.e. toe-in. Similar effect of higher energy consumption as in the cambered wheel will be obtained in this type of misalignment as the mis-aligned wheel needs more work to achieve same goal than when it is normal. The wheel flatness and less air pressure is also another cause of unnecessary losses in wheels, which also can easily be determined by monitoring the wheel torque using the disturbance observer. The commercial vehicles nowadays are having various mechanical system to find out the excessive losses in wheels. These mechanical systems can be replaced by a simple reaction torque observer a variant of the disturbance observer using the current amplifier.

IV. Control

Reaction torque observe is used as a force sensor to continuously monitor the frictional force between the wheel and the ground. The current amplifier was used to command the current to make the system more robust. Using the current amplifier in the system came with another advantage of measuring wheel torques without using any force sensor. The Figure 5 shows the schematic of the reaction torque observer. The properties of brushed DC motor in combination with the current amplifier is used as the force sensor. However, the relationship between the current and the torque of the brushed DC motor is not perfectly linear and the changes with different operating conditions, the RTOB can be tuned to calculate motor torque with high accuracy than in the commercial force sensors.

Reaction torque observer with the disturbance observer was implemented to observe the wheel torque of the system. Figure 6 summarises the control algorithm implemented in the WMR. Here the motor disturbances were compensated

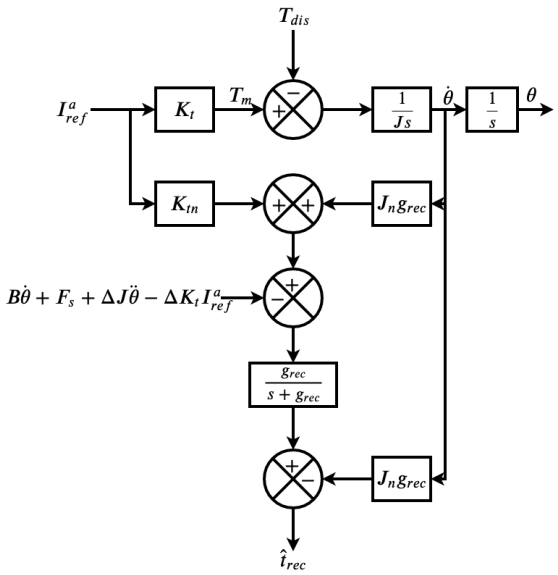

Fig. 5: Torque Command and Reaction Torque Observer (RTOB) for a DC Motor

from the disturbance observer whereas the motor torque was calculated using the reaction torque observer. Velocity and position commands were given, and calculated using the dead reckoning.

V. Experiments and Results

Wheeled mobile robot's were growing in uses everyday. The electrical vehicle were shaping the world into new pollution less transportation. In any of the wheeled mobile robot platform, the alignment of the wheels plays a crucial role not only in stability and controllability but also in energy consumption. Here, in this section, we tried to develop a simple yet very useful method to approximate wheel alignment without any sensors.

To validate the work two wheeled mobile robot (WMR) was designed with 24V planetary gear motors to drive the setup. Motor torque constant K_t and static friction T were experimentally determined.K_t of the motor was found to be 1.4 Nm/A and T was found to be 0.003 Nm. Robber wheels were used to create the system comparable to the electric automobile running in the real world.

All the experiments were done on a polished marble floor inside the laboratory. Two rotary encoders with 400 pulses per revolution were attached to each motor as shown in the Figure 7a. The system was programmed using STM32F429 Discovery development board with 400 microsecond sampling time. WMR was run with different wheel alignment conditions. Initially the setup was run in a normal condition with the load and without the load to observe the changes in torque profiles. Finally the wheels of WMR were misaligned and the experiment was repeated. Figures 7a, 7b and 7c show the WMR with different misaligned conditions. In Figure 7a left wheel was negative 10 degrees cambered. Similarly left wheel was toed-in in Figure 7b with approximate 10 degrees. The robot was run for 6 meters distance on a straight line with constant velocity of 0.2m/s in all the experiments. Finally both the wheels of WMR were 10 degrees toed.in. The Figure 7c shows the WMR with both wheel toed in.

All the Reaction Torque Observer output were recorded in a SD card in real time. After running the mobile platform on above conditions, all the recorded data from both the wheels and robot coordinates were plotted against time. The initial RTOB output contains frictional component like coulomb and viscous frictions along with the torque that creates motion of WMR. The frictional disturbances were experimentally calculated and compensated in the system. Finally the torque profile obtained after the compensation was solely for the driving.

Initially the WMR motors were run in the free wheel condition; without putting any load in the wheel. Figure 8 shows the torque required for the motors to run the only wheel with 0.2m/s in a straight line. The graph shows that the minimal (almost zero) torques were required to rotate the wheels on no load condition with constant velocity.

Driving the free wheel conditions the torque profiles are not perfect straight lines which was due to the momentarily acceleration of the wheel. Figure 8 shows the average of the torque slightly above the zero torque level, which is a error in compensation of the static friction. The WMR then was placed on the ground with similar conditions and run for the same 6 meters on a straight line in X-Direction. The Figure 9 shows the right and left wheel torque profiles when it was run in the ground without any wheel misalignment.

The torque profile obtained was totally different than that we obtained in no load conditions. Here we put a load of 49kg (mass of WMR) to the motors which has resulted in amplification of errors in gear mates and eccentricities. The figure clearly shows the the cyclic pattern of the torque profile. Also the wheels used were rubber and load of 49kg might also have contributed towards the fluctuating torque.

Our experiment was carried out with a sampling time of 400 microsecond and it is almost impossible for the PD controller to make the velocity constant in that fraction of the second. The motor has to accelerates or decelerate within a very small time period to maintain the constant velocity. Which ultimately creates the torque profile to rise and fall by making a sinusoidal waveform with a mean of 0.5Nm.

After recording and plotting the torque profile with no load condition and normal ground running condition, left wheel of the WMR was negative cambered for 10 degrees by rotating wheel and motor assembly by 10 degrees. Again robot's other parameter were left as it is. Running with negative camber; the robot start to feel the horizontal component of force and started to drift horizontally in y direction and comes back to its planned planned orientation after a few seconds. The reordered data with one wheel camber was plotted as shown in Figure 10 in two wheel torque profiles. The graph clearly indicates that there is no significant change in right wheel torque generation. But, the torque profile of the left wheel now has changed and

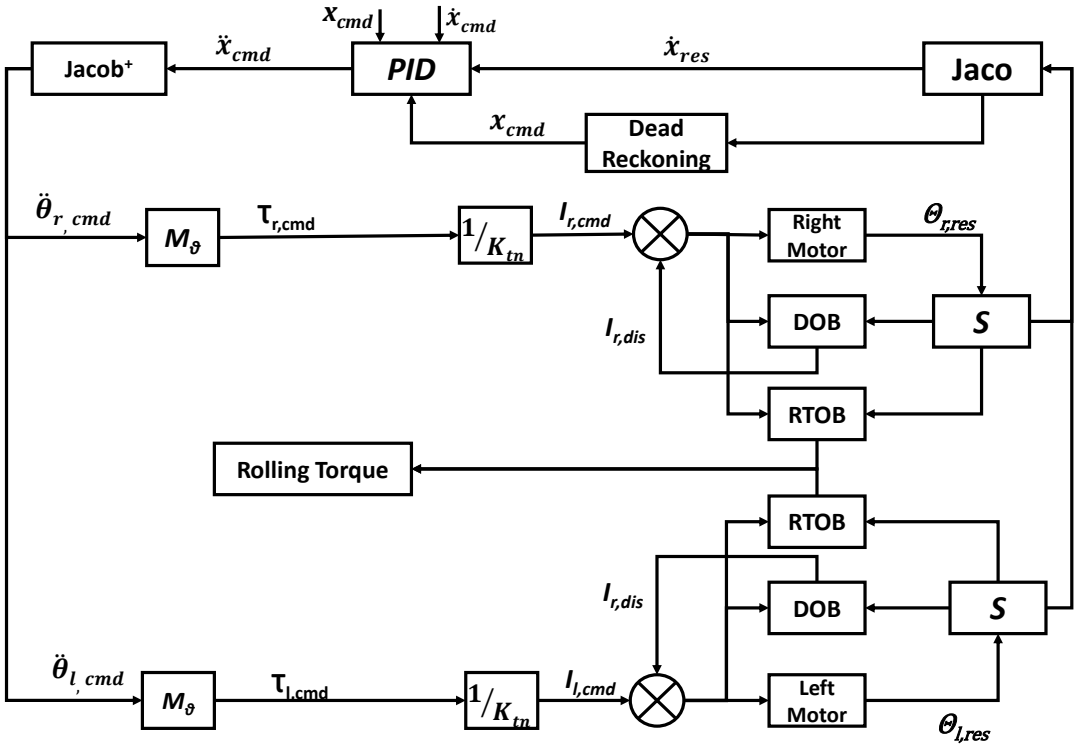

Fig. 6: WMR control flowchart with Disturbance Observer (DOB) as compensator and Reaction Torque Observer (RTOB) as torque observer

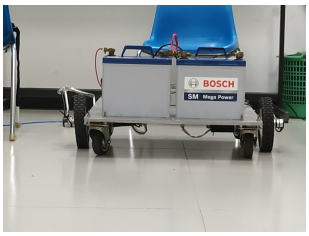

(a) One Wheel Camber

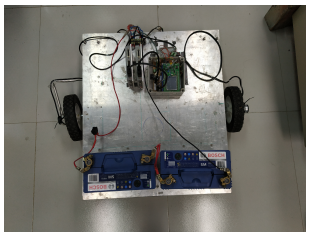

(b) One Wheel TOE IN

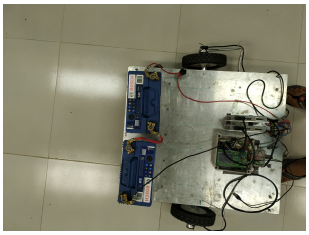

(c) Both Wheel TOE IN

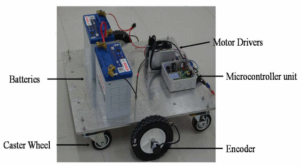

(d) Ordinary WMR

Fig. 7: Different wheel alignment conditions of WMR for experimental runs

the torque generated has increased to almost the double of the normal wheel. This graphs indicates that cambered wheel can easily be detected without any sensor by just comparing the torque profile with and without wheel camber or comparing it with a recorded torque profile.

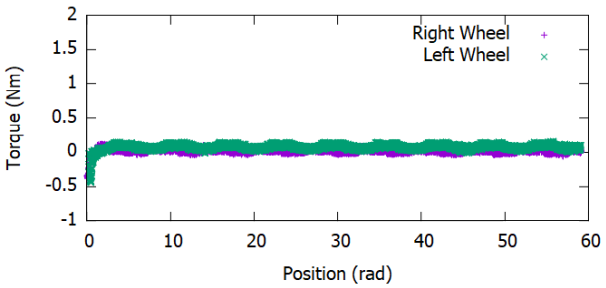

Fig. 8: Wheel Torque Profiles With No Load

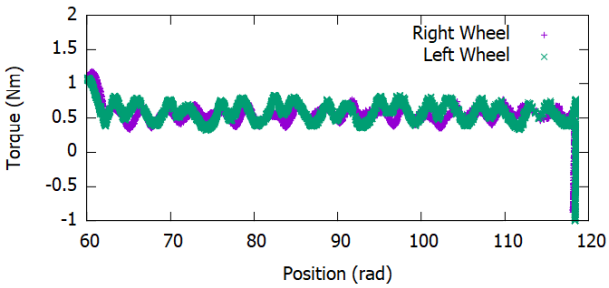

Fig. 9: Wheel Torque Profiles When Ground Moving

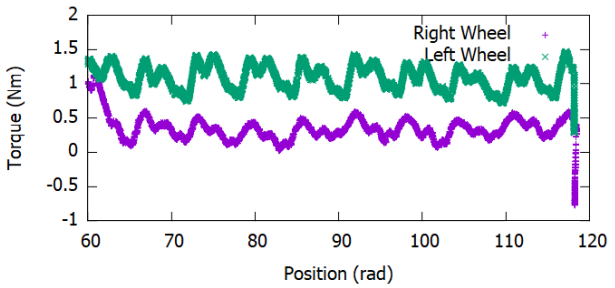

Fig. 10: Wheel Torque Profiles When Left Wheel camber 10 Degrees

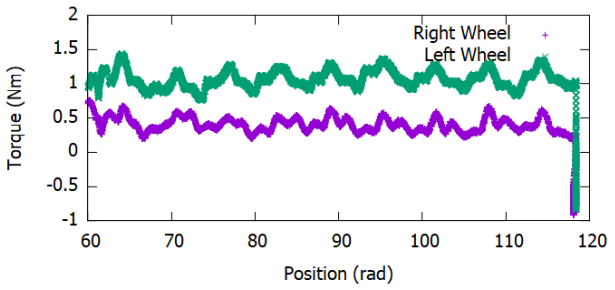

Fig. 11: Wheel Torque Profiles When Left Wheel TOE-IN 10 Degrees

Now, the WMR was changed to TOE-IN condition as shown in Figure 7b and a similar experiment was repeated. Figure 11 shows wheel torque profiles when the left wheel was toed in and run on the ground. The torque generation obtained for the right wheel is sinusoidal with an average torque around 0.5Nm which is similar to that of running on ground without any wheel misalignment. But the left wheel shown in Figure 11 represents the required torque to complete the task that has gone above 1Nm. It is clear that misaligned wheel needs a high torque compered to the normal wheel.

Finally both wheels of WMR were made toe-in 10 degree as shown in Figure 7c. The plotted torque profiles show both the wheel were taking almost double the amount of torque than in a normal WMR.

Figure 12 shows the wheel torque profiles of both wheels of WMR with both wheels with toe-in. From all the experiments we came to know that if we implement DOB and RTOB on a mobile platform or electric vehicles and constantly monitor the torque profiles we can detect wheels problems by using the current consumption. This overdrawn current (excess torque) can be used to estimate wheel misalignments if the vehicle was run in a straight path.

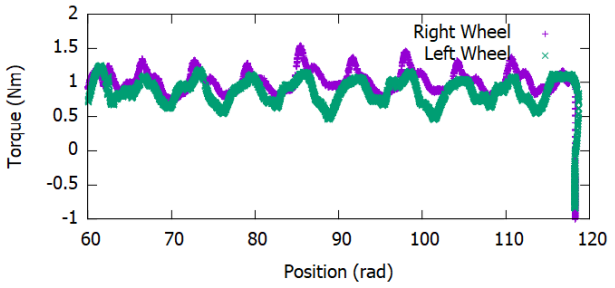

Fig. 12: Wheel Torque Profiles When Both Wheel TOE-IN 10 Degrees

VI. Conclusions

In this work the change of the wheel torque profile with different conditions of wheel alignment was analyzed and a simple way of detecting misalignment was suggested. A Wheeled Mobile Robot (WMR) was developed to implement DOB and the RTOB for position and velocity control. Wheel torques were observed in the real time. In the experiment with the WMR we found a significant change in wheel torque is required to drive the system when wheels with small camber or toe-in. Our work showed a way of detecting fault in wheels without using any sensor by comparing the torque profile required to travel in straight line. Furthermore the purposed method is suitable to be used in electric automobiles as well.

References

[1] Damm, Jurgen. "Method and device for wheel camber adjustment." U.S. Patent No. 7,673,883. 9 Mar. 2010.

[2] Abumi, Takamasa, and Toshiyuki Murakami. "Posture stabilization of two-wheel drive electric motorcycle by slip ratio control considering camber angle." 2015 IEEE International Conference on Mechatronics (ICM). IEEE, 2015.

[3] Xu, He, et al. "Contact angle estimation based on kinematics modeling analyses for rover with caster and camber." 2010 IEEE International Conference on Robotics and Biomimetics. IEEE, 2010.

[4] Yunta, J., et al. "Influence of camber angle on tire tread behavior by an on-board strain-based system for intelligent tires." Measurement 145 (2019): 631-639.

[5] Lamy, Christophe, and Michel Basset. "A vision-based approach to wheel camber angle and tyre loaded radius measurement." Sensors and Actuators A: Physical 161.1-2 (2010): 134-142.

[6] Young, Jieh-Shian, Hong-Yi Hsu, and Chih-Yuan Chuang. "Camber angle inspection for vehicle wheel alignments." Sensors 17.2 (2017): 285.

[7] S. D. A. P. Senadheera and A. M. H. S. Abeykoon, "Sensorless terrain estimation for a wheeled mobile robot," 2017 IEEE International Conference on Industrial and Information Systems (ICIIS), Peradeniya, 2017, pp. 1-6.

[8] Katsura, Seiichiro, Kouhei Ohnishi, and Kiyoshi Ohishi. "Transmission of force sensation by environment quarrier based on multilateral control." 31st Annual Conference of IEEE Industrial Electronics Society, 2005. IECON 2005.. IEEE, 2005.